Soft Mode Doublet in $PbMg_{1/3}Nb_{2/3}O_3$ Relaxor Investigated with Hyper-Raman Scattering

A. Al-Zein,[1,2] J. Hlinka,[3] J. Rouquette,[2] and B. Hehlen[1]

[1]*Laboratoire des Colloides, Verres et Nanomatériaux (LCVN), UMR CNRS 5587, University of Montpellier II, 34095 Montpellier, France*

[2]*Institut Charles Gerhardt, UMR CNRS 5253, University of Montpellier II, 34095 Montpellier, France*

[3]*Institute of Physics, Academy of Sciences of the Czech Republic, Na Slovance 2, 18221 Praha 8, Czech Republic*

(Received 4 February 2010; published 29 June 2010)

Hyper-Raman scattering experiments suggest that a splitting of the lowest F_{1u}-symmetry mode of $PbMg_{1/3}Nb_{2/3}O_3$ crystal occurs in a wide temperature range around its Burns temperature $T_d \approx 630$ K. The upper-frequency component, earlier investigated by inelastic neutron scattering experiments above T_d, appears to be *underdamped* even hundred of degrees *below* T_d. The lower-frequency component, known below T_d from far-IR spectroscopy, actually *becomes underdamped above* T_d. This suggests that the lower-frequency mode is the ''primary'' polar soft mode of $PbMg_{1/3}Nb_{2/3}O_3$, responsible for the Curie-Weiss behavior of its dielectric permittivity above T_d.

DOI: 10.1103/PhysRevLett.105.017601 PACS numbers: 77.80.−e, 63.20.−e, 78.30.−j

Lead magnesium niobate crystal $PbMg_{1/3}Nb_{2/3}O_3$ (PMN) is considered as a model system of ferroelectric relaxors. It has a perovskite structure of general formula ABO_3 with an average $Pm\bar{3}m$ (O_h^1) cubic symmetry down to the lowest temperature. At the same time, the broad and frequency-dependent maximum of the dielectric constant $\epsilon(T)$ suggests a ''diffuse'' ferroelectric phase transition at around 400 K. At the nanometric scale, the crystal obviously has a lower symmetry owing to the *B*-site compositional local ordering of Mg^{2+} and Nb^{5+} ions ($Fm\bar{3}m$-type clusters) and to the off-site ionic displacements. Although the ferroelectric state was achieved only in samples field-cooled below the freezing temperature $T_f \approx 220$ K, it is believed that a sort of randomly oriented ferroelectric clusters (polar nanoregions) can start to play a considerable role already below the Burns temperature [1] $T_d \approx 630$ K, where one observes deviations from the Curie-Weiss law of $\epsilon(T)$ [2] and from the linear temperature dependence of the refractive index $n(T)$ [1]. It was recently argued that other quantities like thermal expansion show similar departures from the usual temperature dependence at still another characteristic temperature T^*. Interestingly, temperature dependence of acoustic emission from PMN crystals shows two quite sharp peaks near 500 and 630 K correlating fairly well with the temperatures T^* and T_d [3,4].

The zone-center polar soft mode, a hallmark of every displacive ferroelectric phase transition, has been obviously already searched by all available techniques, including Raman scattering [5]. In PMN, an excitation with a low and strongly temperature-dependent frequency has been first identified by inelastic neutron scattering (INS) investigations [6–8] but only above T_d and below T_f. The same mode has been then also seen by IR reflectivity and transmission spectroscopy experiments in PMN crystals at low temperatures [9] and in PMN thin films even up to the Burns temperature [10]. The nature of this mode in the intermediate ''waterfall'' region between T_f and T_d in bulk PMN has been strongly debated: The INS spectra were compatible with a presence of an overdamped zone-center soft mode, but the available data did not allow a unique determination of its frequency and damping parameter [11].

At the same time, the presence of another mode was argued [6,12], at least above T_d, because the observed soft mode showed a Cochran law $\omega_0^2 \propto (T - T_0)$ with $T_0 \approx 0$ K [8] or even negative [12] above T_d, while $T_0 \approx +400$ K was expected from the high-temperature Curie-Weiss law [2]. Indeed, PMN should behave like a usual ferroelectric above T_d, and the dielectric permittivity should be thus determined mostly by a corresponding soft polar excitation. In fact, the INS spectra could be alternatively fitted to a two-mode model considering an additional, so-called quasioptic mode, having frequency as low as ~ 12 cm^{-1} at 880 K and $T_0 \approx +340$ K above T_d, but the fit was clearly not unique since the single damped harmonic oscillator (DHO) model worked equally well [8]. Later on, an additional polar excitation, originally denoted as a ''central mode,'' has been directly evidenced as a separate dielectric loss peak at about 20 cm^{-1} by IR and terahertz spectroscopy. It was proposed that the two polar excitations could correspond to the soft-mode fluctuations parallel and perpendicular to the local field, respectively [13]. Therefore, the two polar modes (the partially soft mode and the central mode) were tentatively denoted as A_1 and E_1 components of the TO1 soft mode [13]. However, the E_1 central mode could not be followed above T_d by the IR technique because of the strong absorption in the far-IR region.

Hyper-Raman scattering (HRS) provides an interesting alternative to study the vibrations in ferroelectric-type materials and, in particular, the paraelectric soft modes [14]. The simple O_h^1 ($Z = 1$) perovskite structure has four zone-center optic modes, three F_{1u} polar modes and one F_{2u} nonpolar vibration, all being triply degenerated

and active in HRS. Surprisingly, the HRS spectroscopy has only been little exploited in ferroelectric relaxors [15–17]. The advantage of HRS for the measurement of soft modes is apparent from Fig. 1(a), where the low frequency part of the HRS spectrum of PMN is compared to a zone-center INS spectrum [12]. In the latter, the leakage of the elastic scattering and of the scattering by acoustic phonons considerably limits the observations at low frequencies. On the contrary, the very good instrumental resolution combined with a very weak second harmonic generation signal above T^* [narrow band at $\omega = 0$ in Fig. 1(a)] allows measurements of polar modes by HRS down to a few cm^{-1}.

HRS experiments have been performed by using the setup described in Ref. [17]. The sample was a 1-mm-thick platelet of PMN single crystal grown at Shanghai Institute of Ceramics, with [001] (z axis) normal to the surface. It was mounted in a hot stage with the [100] (x) and [010] (y) crystallographic axes parallel to the horizontal (H) and vertical (V) direction, respectively. The data were collected in the backscattering geometry with $q \parallel [001]$. A broadband half-plate wave followed by a Glan-Thomson polarizer allowed for an analysis of the scattered light polarized along V or H. Following the standard notation [18], VVV spectra thus correspond to a $z(y, yy)\bar{z}$ scattering geometry and HVV spectra to $z(x, yy)\bar{z}$. An 1800 grooves/mm grating and a 150 μm entrance slit give rise to a resolution of $\sim 3\ \mathrm{cm}^{-1}$. Cooling and heating rates did not exceed 10 K/min with a stabilization temperature within $\sim \pm 1$ K.

Figure 1(b) shows a series of HRS spectra measured between 520 and 750 K without polarization analysis in the frequency region where the F_{1u}(TO1) mode is expected to contribute. Clearly, there are two bands there in the whole temperature interval investigated. The upper-frequency band peaks near 45 cm^{-1} at all temperatures, while the lower-frequency band exhibits a clear soft-mode behavior on cooling. Around T_d, it transforms into a gradually narrowing quasi-elastic-like feature, which then merges with more and more intense second harmonic generation elastic scattering around about 500 K [inset in Fig. 1(b)]. The doublet appears in both VVV and HVV polarized HRS spectra (Fig. 2). This supports the assumption that both modes are related to the F_{1u} mode, active in both geometries, rather than to the F_{2u} [15], which should be absent in the VVV spectrum [17]. Therefore, it is natural, in the spirit of Ref. [13], to associate the upper- and lower-frequency band as A_1 and E_1 components of the $F_{1u}(TO1)$ mode, respectively [see Fig. 1(a)].

For a given phonon mode, one finds the hyper-Raman intensity [19]

$$I_{\mathrm{HRS}} \propto \left(\frac{\omega_S^4}{\omega}\right)[n(\omega) + 1]F(\omega)\sum_{\delta}|e_i^S R_{ijk}^{\delta} e_j^L e_k^L|^2, \quad (1)$$

where $\omega_S = 2\omega_L \pm \omega$ is the frequency of the scattered field, $n(\omega)$ is the Bose-Einstein population factor, and $F(\omega)$ is the normalized response function of the mode. $\mathbf{e^L}$ and $\mathbf{e^S}$ are the polarization vectors of the incident (L) and detected (S) photons, respectively. The index δ distinguishes different HRS tensors R_{ijk}^{δ} of a degenerate mode. The spectra were fitted to a model including a flat background, a narrow Gaussian function accounting for the second harmonic generation elastic scattering, and two DHOs standing for the E_1 and the A_1 modes, each de-

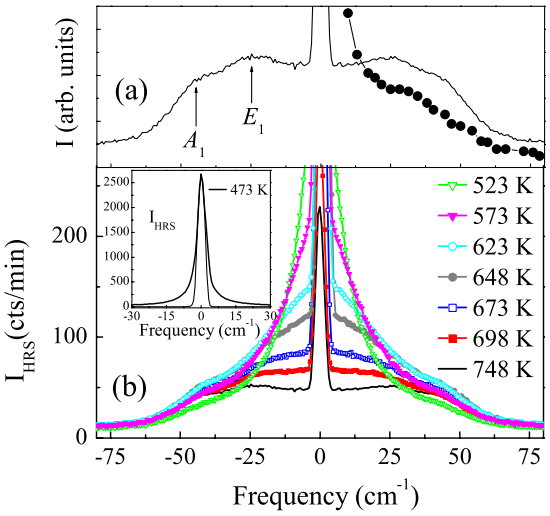

FIG. 1 (color online). (a) Unpolarized (V + H) HRS spectra of PMN at 748 K compared with INS data at 750 K taken from Ref. [12] (●). (b) Temperature evolution of unpolarized HRS PMN spectra. Inset : 473 K spectra together with the instrumental function (thin line).

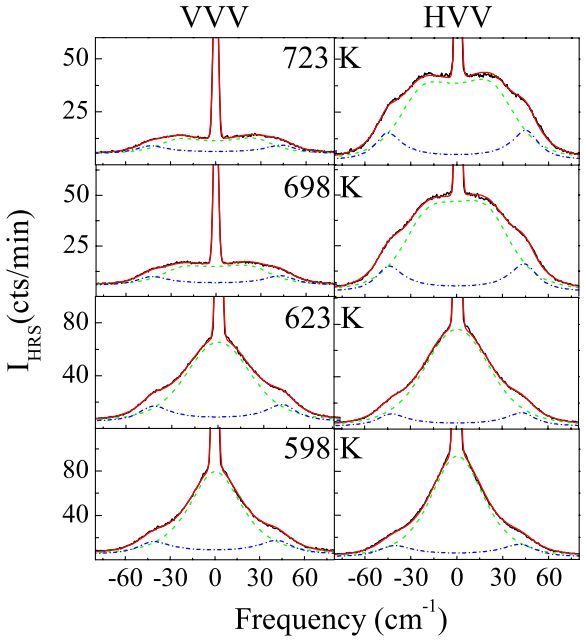

FIG. 2 (color online). VVV (left) and HVV (right) hyper-Raman spectra of PMN at various temperatures fitted to the model described in the text (full lines). Dashed and dash-dotted lines show DHO components corresponding to the E_1 and the A_1 modes, respectively.

scribed by $F(\omega) = (2\omega/\pi)\,\mathrm{Im}[1/(\omega_0^2 - \omega^2 - i\Gamma\omega)]$, where ω_0 and Γ are DHO frequency and damping, respectively. The model very nicely reproduce the experimental data in the full temperature range explored (Fig. 2), and the values of ω_0 and Γ obtained from VVV and HVV spectra are very similar. The averaged values of ω_0 and Γ are displayed in Fig. 3.

Let us note that, in our fitting model, the DHO associated with E_1 mode plays a dominant role: It describes the majority of the scattering intensity, and it shows a pronounced softening on cooling. In fact, its peak frequency is zero below T_d (Fig. 2). In classical soft-mode works [20], such a mode is denoted as an *overdamped* mode, as opposed to an *underdamped* mode having its scattering spectrum peaked at a nonzero frequency. The observed overdamping-underdamping crossover suggests that the E_1 mode is responsible for the difficulties in the analysis of the INS spectra between T_f and T_d: The peak frequency of the E_1 mode could not be well resolved in early INS data. At the same time, it is the A_1 mode frequency which coincides with the soft-mode frequency proposed from the INS spectra taken above T_d [7]. This suggests that the A_1 mode corresponds to the vibration that was previously assigned to the soft mode of PMN [7]. However, in contrast with the earlier anticipations [7], this mode does not show any signature of overdamping below T_d.

The DHO model is very useful for the description of lattice modes with relatively large damping parameters. In the high-temperature limit, the maxima of the one-phonon DHO scattering spectral function $S(\omega) = [n(\omega) + 1]\,\mathrm{Im}[1/(\omega_0^2 - \omega^2 - i\Gamma\omega)]$ are at $\omega' = \pm\sqrt{\omega_0^2 - \Gamma^2/2}$ if $\omega_0 > \Gamma/\sqrt{2}$ and there is only one maximum at $\omega = 0$ if $\omega_0 < \Gamma/\sqrt{2}$. A similar quantity is the frequency $\omega'' = \pm\sqrt{\omega_0^2 - \Gamma^2/4}$, defining the periodic factor in the temporal response of the oscillator coordinate Q in the absence of driving forces $Q(t) = e^{-t\Gamma/2}\cos(\omega'' t + \phi)$ for $(\omega_0 > \Gamma/2)$. Frequencies ω' and ω'' calculated by using the E_1 mode parameters tend to zero at temperatures $T_{OD} = 670$ K and $T_{CD} = 580$ K marking overdamping and critical damping of the E_1 mode, respectively [Fig. 4(a)]. Both T_{OD} and T_{CD} are quite close to T_d.

It is well known that an independent experimental determination of ω_0 and Γ from the $S(\omega)$ line shape of an overdamped mode is quite problematic. Therefore, the spectra *below* T_d were fitted with the E_1 mode damping fixed to the value obtained by linear extrapolation of $\Gamma(T)$ measured *above* T_d (see the inset in Fig. 3). Still, the most reliable spectral parameter of a strongly overdamped DHO is the relaxational frequency $\omega_{rel} = \omega_0^2/\Gamma$, corresponding to the half width at half maximum [21] of its $S(\omega)$. Since ω_{rel} of the E_1 mode clearly tends to zero at about 400 K [Fig. 4(a)], we are confident that also ω_0^2 does so. Indeed, a fit of ω_0 with a Cochran law gives $T_0 \cong 390 \pm 30$ K [Figs. 3 and 4(a)]. These observations are a very strong indication that the E_1 mode observed here accounts for the Curie-Weiss temperature T_0 extrapolated from $\epsilon(T)$ at high temperature [2].

In fact, well above T_d, where one can rely on the ω_0 value of the E_1 mode, the dielectric contribution of the soft

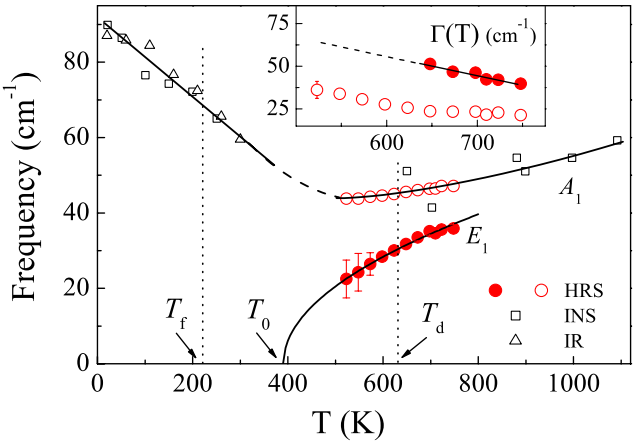

FIG. 3 (color online). Temperature dependence of E_1 and A_1 frequencies ω_0 and damping (in the inset) compared to the INS data of Refs. [7,8] and IR of Ref. [9]. The lower line (E_1) corresponds to a fit with a Cochran law.

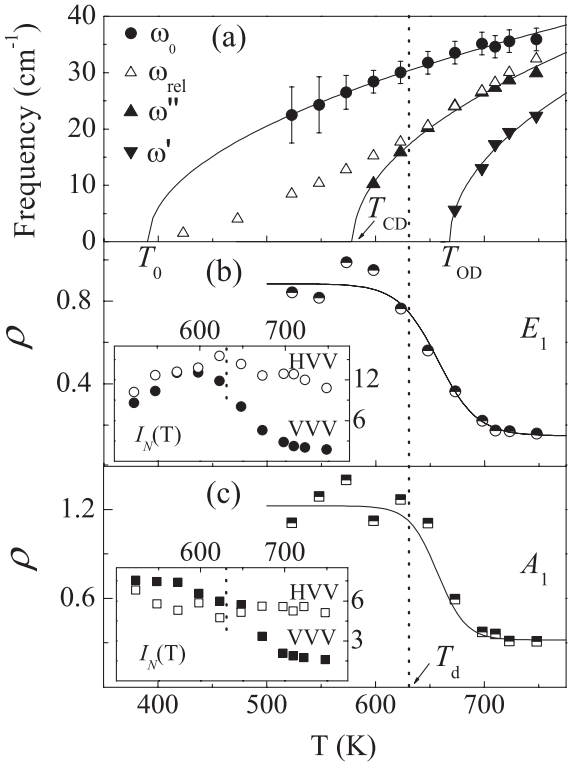

FIG. 4. Top: Temperature dependence of the E_1 mode frequencies ω_0, ω_{rel}, ω', and ω'', defined in the text. The lines stand for a Cochran-like law $\omega^2 \propto (T - T_0)$. (b) and (c) show the polarization ratio ρ of the normalized HRS intensities of the E_1 and A_1 components, respectively. The lines are guides for the eyes. Insets show I_N(VVV) (full symbols) and I_N(HVV) (open symbols) for the two components separately.

doublet can be estimated directly. By using the mode-*plasma* frequencies $\Omega[A_1] = 537\ \mathrm{cm}^{-1}$ and $\Omega[E] = 711\ \mathrm{cm}^{-1}$ of the A_1 and E components of the $PbTiO_3$ soft mode [22] and the ω_0 frequencies of the A_1 and E_1 components of the PMN soft mode at 748 K (47.2 and 35.9 cm^{-1}, respectively), one can estimate the average static dielectric contribution of these two modes as

$$\Delta\epsilon = \frac{1}{3}\left(\frac{\Omega[A_1]}{\omega_0[A_1]}\right)^2 + \frac{2}{3}\left(\frac{\Omega[E]}{\omega_0[E_1]}\right)^2 \approx 305. \qquad (2)$$

This value [23] is still much larger than the background permittivity $\epsilon_\infty \approx 25$ associated with the TO2 and TO3 polar modes and electronic contributions [13], and the total static permittivity $\epsilon_\infty + \Delta\epsilon \approx 330$ is thus in an excellent agreement with the low frequency permittivity $C/(T - T_0) \approx 343$, evaluated at $T = 748$ K by using the Curie-Weiss temperature $T_0 = 398$ K and Curie constant $C = 1.2 \times 10^5$ K from Ref. [2].

The pairs of HVV and VVV spectra were recorded at identical conditions, and slight intensity drifts during temperature changes were corrected by using the Bose-factor-corrected HVV intensity of the very stable F_{2u} mode at $\sim 248\ \mathrm{cm}^{-1}$ [17]. Therefore, we could extract for each mode its relative intensity factor I_N, proportional to the sum of squares of the HRS tensor components given in the right-hand side of Eq. (2). Results show that the E_1 mode has twice as large I_N than the A_1 mode as one may expect for a doublet-singlet pair derived from the same parent F_{1u}(TO1) mode [insets in Fig. 4(b) and 4(c)]. At the same time, I_N(VVV) and the polarization ratio $\rho = I_N(\mathrm{VVV})/I_N(\mathrm{HVV})$ are convincingly enhanced for both phonon modes near T_d [Fig. 4(b) and 4(c)]. It suggests that the R_{111} tensor element of the parent F_{1u}(TO1) mode is particularly sensitive to a local structural change. These observations might relate to the growth of a local-polarization-related order parameter near T_d.

In summary, the current HRS experiment helped to elucidate ferroelectric order-parameter dynamics in the paraelectric phase of a PMN single crystal. In particular, our data are well described by a model where (i) the scattering response has two components in a broad range of temperatures both below and above the Burns temperature, (ii) the E_1 mode becomes underdamped above the Burns temperature, and (iii) the observed doublet is responsible for the high-temperature Curie-Weiss law. Moreover, both modes disclose a pronounced increase of parallel-polarized HRS intensity below T_d, possibly indicating the onset of the local ferroelectric order, while the E_1 mode clearly softens towards the anticipated random field transition [24] T_0. We hope that these results will help to approach a more coherent picture of the dynamical polarization correlations in relaxors in general.

This work was supported by the Czech Science Foundation Project No. P204/10/0616 and the AVOZ10100520 project.

Note added in proof.—Manifestation of the two soft modes in INS spectra has been recently revisited also in Ref. [25].

[1] G. Burns and F. H. Dacol, Solid State Commun. **48**, 853 (1983).
[2] D. Viehland, S. J. Jang, L. E. Cross, and M. Wuttig, Phys. Rev. B **46**, 8003 (1992).
[3] E. Dul'kin, I. P. Raevskii, and S. M. Emel'yanov, Phys. Solid State **45**, 158 (2003).
[4] B. Dkhil, P. Gemeiner, A. Al-Barakaty, L. Bellaiche, E. Dul'kin, E. Mojaev, and M. Roth, Phys. Rev. B **80**, 064103 (2009).
[5] O. Svitelskiy, J. Toulouse, G. Yong, and Z.-G. Ye, Phys. Rev. B **68**, 104107 (2003); D. Fu, H. Taniguchi, M. Itoh, S.-Y. Koshihara, N. Yamamoto, and S. Mori, Phys. Rev. Lett. **103**, 207601 (2009).
[6] A. Naberezhnov, S. Vakhrushev, B. Dorner, D. Strauch, and H. Moudden, Eur. Phys. J. B **11**, 13 (1999).
[7] P. M. Gehring, S. Wakimoto, Z.-G. Ye, and G. Shirane, Phys. Rev. Lett. **87**, 277601 (2001).
[8] S. Wakimoto, C. Stock, R. J. Birgeneau, Z.-G. Ye, W. Chen, W. J. L. Buyers, P. M. Gehring, and G. Shirane, Phys. Rev. B **65**, 172105 (2002).
[9] V. Bovtun, S. Kamba, A. Pashkin, M. Savinov, P. Samoukhina, J. Petzelt, I. P. Bykov, and M. D. Glinchuk, Ferroelectrics **298**, 23 (2004).
[10] S. Kamba, M. Kempa, V. Bovtun, J. Petzelt, K. Brinkman, and N. Setter, J. Phys. Condens. Matter **17**, 3965 (2005).
[11] J. Hlinka and M. Kempa, Phase Transit. **81**, 491 (2008).
[12] S. B. Vakhrushev and S. M. Shapiro, Phys. Rev. B **66**, 214101 (2002).
[13] J. Hlinka, T. Ostapchuk, D. Noujni, S. Kamba, and J. Petzelt, Phys. Rev. Lett. **96**, 027601 (2006).
[14] H. Presting, J. A. Sanjurjo, and H. Vogt, Phys. Rev. B **28**, 6097 (1983).
[15] H. Hellwig, A. Sehirlioglu, D. A. Payne, and P. Han, Phys. Rev. B **73**, 094126 (2006).
[16] B. Hehlen, G. Simon, and J. Hlinka, Phys. Rev. B **75**, 052104 (2007).
[17] A. Al-Zein, B. Hehlen, J. Rouquette, and J. Hlinka, Phys. Rev. B **78**, 134113 (2008).
[18] V. N. Denisov, B. N. Marvin, and V. B. Podobedov, Phys. Rep. **151**, 1 (1987).
[19] H. Vogt, Phys. Rev. B **38**, 5699 (1988).
[20] M. DiDomenico, Jr., S. H. Wemple, S. P. S. Porto, and R. P. Bauman, Phys. Rev. **174**, 522 (1968).
[21] Data points for ω_{rel} below 500 K were determined from HWHM corrected by instrumental resolution.
[22] J. Hlinka, J. Petzelt, S. Kamba, D. Noujni, and T. Ostapchuk, Phase Transit. **79**, 41 (2006).
[23] Similar results ($\Delta\epsilon \approx 335$) were obtained by using plasma frequency estimates inferred from room-temperature reflectivity spectra of PMN itself (Table 11 of Ref. [22]).
[24] R. A. Cowley, S. N. Gvasaliya, and B. Roessli, Ferroelectrics **378**, 53 (2009).
[25] S. B. Vakhrushev, R. G. Burkovsky, S. Shapiro, and A. Ivanov, Phys. Solid State **52**, 889 (2010).